

Optical multi-hysteresis and quasi-solitons in nonlinear plasma

A. E. Kaplan *

Electr. and Comp. Eng. Dept., The Johns Hopkins University, Baltimore, MD 21218, US

alexander.kaplan@jhu.edu

Abstract: An overdense plasma layer irradiated by intense light can exhibit dramatic nonlinear-optical effects due to a relativistic mass-effect of free electrons: highly-multiple hysteresis of reflection and transition, and emergence of immobile waves of large amplitude. Those are trapped quasi-soliton spikes sustained by a weak pumping having a tiny fraction of their peak intensity once they have been excited first by higher power pumping. The phenomenon persists even in the layers with "soft", wash-out boundaries, as well as in a semi-infinite plasma with low absorption.

© 2013 Optical Society of America

OCIS codes: (190.0190) Nonlinear optics; (190.1450) Optical bistability; (190.6135) Spatial solitons; (350.5720) relativity .

References and links

1. A. E. Kaplan, "Hysteresis reflection and refraction by nonlinear boundary - a new class of effects in nonlinear optics," *JETP Lett.* **24**, 114-119 (1976).
2. A. E. Kaplan, "Theory of hysteresis reflection and refraction of light by a boundary of a nonlinear medium," *Sov. Physics JETP* **45**, 896-905 (1977).
3. P. W. Smith, J. P. Hermann, W. J. Tomlinson, and P. J. Maloney, "Optical bistability at a non-linear interface," *Appl. Phys. Lett.* **35**, 846-848 (1979).
4. P. W. Smith, W. J. Tomlinson, P. J. Maloney, and J. P. Hermann, "Experimental studies of a non-linear interface," *IEEE JQE* **17**, 340-348 (1981).
5. P. W. Smith and W. J. Tomlinson, "Nonlinear optical interfaces – switching behavior," *IEEE JQE* **20**, 30-36 (1984).
6. S. De Nicola, A. E. Kaplan, S. Martellucci, P. Mormile, G. Pierattini, and J. Quartieri, "Stable hysteretic reflection of light at a nonlinear interface," *Appl. Phys. B* **49**, 441-444 (1989).
7. A. I. Akhiezer and R. V. Polovin, "Theory of wave motion of an electron plasma" *Sov. Phys. JETP-USSR*, **3**, 696-705 (1956).
8. C. Max and F. Perkins, "Strong electromagnetic waves in overdense plasmas" *Phys. Rev. Lett.*, **27**, 1342-1345 (1971).
9. J. H. Marburger and R. F. Tooper, "Nonlinear optical standing waves in overdense plasmas", *Phys. Rev. Lett.*, **35**, 1001-1004 (1975).
10. S. V. Bulanov, I. N. Inovenkov, V. I. Kirsanov, N. M. Naumova, and A. S. Sakharov, "Nonlinear depletion of ultrashort and relativistically strong laser pulses in an underdense plasma," *Phys. Fluids B* **4**, 1935-1942 (1992).
11. T. Z. Esirkepov, F. F. Kamenets, S. V. Bulanov, and N. M. Naumova, "Low-frequency relativistic electromagnetic solitons in collisionless plasmas," *JETP Lett.* **68**, 36-41 (1998).
12. M. Tushentsov, A. Kim, F. Cattani, D. Anderson, and M. Lisak, "Electromagnetic energy penetration in the self-induced transparency regime of relativistic laser-plasma interactions," *Phys. Rev. Lett.* **87**, 275002 (2001).
13. T. Esirkepov, K. Nishihara, S. V. Bulanov, and F. Pegoraro, "Three-dimensional relativistic electromagnetic sub-cycle solitons," *Phys. Rev. Lett.* **89**, 275002 (2002).
14. G. Lehmann, E. W. Laedke, and K. H. Spatckek, "Two-dimensional dynamics of relativistic solitons in cold plasmas," *Phys. Plasma* **15**, 072307 (2008) and references therein
15. G. A. Mourou, T. Tajima, and S. V. Bulanov, "Optics in the relativistic regime," *Rev. Mod. Phys.* **78**, 309-371 (2006), and references therein.
16. W. Chen and D. L. Mills, "Gap solitons and the nonlinear optical response of superlattices," *Phys. Rev. Lett.* **58**, 160-163 (1987).

17. J. E. Sipe and H. G. Winful, "Nonlinear Schroedinger solitons in periodic structure," *Opt. Lett.* **13**, 132-133 (1988).
18. D. N. Christodoulides and R. I. Joseph, "Slow Bragg solitons in nonlinear periodic structures," *Phys. Rev. Lett.* **62**, 1746 (1989).
19. B. J. Eggleton, R. E. Slusher, C. M. de Sterke, P. A. Krug, and J. E. Sipe, "Bragg grating solitons," *Phys. Rev. Lett.* **76**, 1627-1630 (1996).
20. D. Mandelik, H. S. Eisenberg, Y. Silberberg, R. Morandotti, and J. S. Aitchison, "Observation of mutually trapped multiband optical breathers in waveguide arrays," *Phys. Rev. Lett.* **90**, 053902 (2003).
21. O. Zobay, S. Potting, P. Meystre, and E. M. Wright, "Creation of gap solitons in Bose-Einstein condensates," *Phys. Rev. A* **59**, 643-648 (1999).
22. H. G. Winful and J. H. Marburger, "Hysteresis and optical bistability in degenerate four-wave mixing", *Appl. Phys. Lett.*, **36**, 613-614 (1980).
23. A. E. Kaplan and C. T. Law, "Isolas in four-wave mixing optical bistability," *IEEE J. Quant. Electr.*, **QE-21**: 1529-1537 (1985).
24. D. J. Gauthier, M. S. Malcut, A. L. Gaeta, R. W. Boyd, "Polarization bistability of counterpropagating laser beams", *Phys. Rev. Lett.* **64**, 1721-1724 (1990)
25. A. E. Kaplan and Y. J. Ding, "Hysteretic and multiphoton optical resonances of a single cyclotron electron," *IEEE JQE* **24**, 1470-1482 (1988), and references therein.
26. A. V. Korzhimanov, V. I. Eremin, A. V. Kim, and M. R. Tushentsov, "Interaction of relativistically strong electromagnetic waves with a layer of overdense plasma," *J. Expr. Theor. Phys.*, **105**, 675-686 (2007)
27. A. E. Kaplan, "Hysteresis in cyclotron resonance based on weak-relativistic mass-effect of the electron," *Phys. Rev. Lett.* **48**, 138-141 (1982).
28. G. Gabrielse, H. Dehmelt, and W. Kells, "Observation of a relativistic bistable hysteresis in the cyclotron motion of a single electron," *Phys. Rev. Lett.* **54**, 537-539 (1985).
29. A. E. Kaplan, "Relativistic nonlinear optics of a single cyclotron electron," *Phys. Rev. Lett.* **56**: 456-459 (1986).
30. A. E. Kaplan and P. L. Shkolnikov, "Lasetron: a proposed source of powerful nuclear-time-scale electromagnetic bursts," *Phys. Rev. Lett.* **88**, 074801(1-4), (2002).
31. R. J. Noble, "Plasma wave generation in the beat-wave accelerator," *Phys. Rev. A* **32**, 460-471 (1985).
32. A. B. Shvartsburg, "Resonant Joule phenomena in a magnetoplasma", *Phys. Reports*, **125**, 187-252 (1985)
33. B. M. Ashkinadze and V. I. Yudson, "Hysteretic microwave cyclotron-like resonance in a laterally confined two-dimensional electron gas," *Phys. Rev. Lett.* **83**, 812-815 (1999).
34. G. Shvets, "Beat-wave excitation of plasma waves based on relativistic bistability," *Phys. Rev. Lett.* **93**, 195004 (2004).
35. B. Ya. Zeldovich, "Nonlinear optical effects and the conservation laws," *Brief Comm. Physics, Lebedev Inst. (FIAN), Moscow* **2**(5), 20-25 (1970).
36. H. M. Gibbs, S. L. McCall, and T. N. C. Venkatesan, "Differential gain and bistability using a sodium-filled Fabri-Perot interferometer," *Phys. Rev. Lett.* **36**, 1135-1138 (1976).
37. This suggests an explanation of a hysteresis lacking in [5]: an artificial nonlinearity used there was due to small dielectric particles suspended in a liquid and had large dissipation because of strong light scattering, vs the experiments [3,4,6] with nearly transparent fluids.
38. A. E. Kaplan, "Gradient marker" – a universal wave pattern in inhomogeneous continuum", *Phys. Rev. Lett.*, **109**, 153901(1-5) (2012)
39. G. A. Askaryan, "Effects of the gradient of a strong electromagnetic beam on electrons and atoms" *Sov. Phys., JETP-USSR*, **15**, 1088-1090 (1962).
40. V. I. Bespalov and V. I. Talanov, "Filamentary structure of light beams in nonlinear liquids" *JETP Lett.* **3**, 307-310 (1966).

1. Introduction

Diverse phenomena such as light reflection at a dielectric interface, under-barrier scattering of an electron in quantum mechanics, and wave propagation in waveguides, plasma, free-electron gas, and in band-gap materials, including Bose-Einstein condensate (BEC), exhibit a common critical behavior: a dramatic transition at a crossover from a traveling wave in an underlying medium to a non-propagating, evanescent wave that carry no energy. The crossover occurs in optics at the angle of total internal reflection at a dielectric interface, at a laser frequency near either a plasma frequency, or a waveguide cut-off frequency, or band-gap edge of a material; in quantum mechanics for electron scattering at the energy close to a potential plateau, etc. It can be of great significance to *nonlinear* optics: a nonlinear refractive index can cause a phase-transition-like effect, since a small light-induced change may translate into a switch from full

reflection to full transmission, resulting in a huge hysteresis. Predicted in [1,2] for nonlinear interfaces, it was explored experimentally in [3-6], with an inconclusive outcome, with some of the experiments [3,4,6] showing a clear hysteresis, while [5] showing none (see also below, Sect. 6). 2D numerical simulations were not well suited then for hysteresis modeling; their very formulation ruled out multivalued outcome by using single-valued boundary conditions.

Here we show, however, that even the most basic, 1D-case, reveals a large phenomenon of highly-hysteretic nonlinear EM-propagation related to the excitation of trapped quasi-solitons (QS's) with intensity exceeding the incident one by orders of magnitude. Even a slight nonlinearity due to the most fundamental mechanism – relativistic (RL) mass-effect of free electrons – suffices to initiate the effect. Multiple (up to hundreds) hysteretic jumps between almost full reflection and full transparency may occur as the laser intensity is swept up and down.

We treat the problem here in a plasma context on account of recent interest in high-intensity laser-plasma interactions and fundamental nature of RL-nonlinearity, but the approach is valid for other crossover problems. An interest to the interaction of strong radiation with plasma excited to relativistic (RL) electron energies goes far back [7-9]. Temporal RL-solitons, in particular in plasma, have also been considered in detail in the literature [10-15]; close to those of underdense plasma are the so called Bragg or band-gap solitons [16-20], including those in BEC [21]. The difference in this work is made by multi-hysteresises (and *standing, immobile* quasi-solitons instead of propagating ones) due to self-induced retro-reflection. The new property is that for the *same incident power* an EM-wave can penetrate into a nonlinear material to *different depths* – varying by orders of magnitude – depending of the history of pumping. We assume a stationary, *cw*, or long pulse mode, and use only RL-nonlinearity in a cold plasma. While this model is greatly simplified *vs* various kinetic approaches, it allows us to keep the basic features necessary to elucidate new results, and have the theory applicable to other systems. Remarkably, even a few- λ -thick plasma layer can produce the effect, so that the absorption and diffraction of light (including nonlinear self-focusing) would be unlikely to significantly affect the propagation. Indeed, the lowest thickness of the layer needed to observe the effect is of the same order as the size of single soliton formed in the layer for a given a normalized detuning from critical frequency δ , which is $\sim \lambda / \pi \sqrt{2\delta}$, see Eq. (13) below. Even in the case of low-intensity soliton, with $\delta = 10^{-4}$, one has that size amounting to $\approx 0.225\text{mm}$ at $\lambda \approx 10\mu\text{m}$ (CO_2 laser), which is far below characteristic absorption or self-focusing scales.

Multi-stability and multi-hysteresises are known to exist in other nonlinear-optical systems, such as e. g. in four-wave mixing [22-24], i. e. in counterpropagating nonlinear waves (with [22] demonstrating first the existence of bistability, while [23] found multi-stable modes observed in experiment later in [24]) and even for a single relativistic electron [25]. A recent work [26] studied steady-state solutions in a 1D plasma layer with sharp boundaries to great degree similar to one of the configurations considered by us here, and stated the existence of multi-valued solutions that are due to a "self-organized" resonances; yet, no explicit hysteresises, nor their characteristics, total number, etc., transpired from that study. It was pointed out however in [26] (p. 677) that some solutions of the major equations used in [26], are unphysical by producing a negative density of electrons, and the procedure of fitting the "physical" parts of the solution to each other and eliminating the meaningless ones, was not based on the theory used. None of these issues came up in our either analytical or numerical calculations made in a consistent way, and our results that can be compared to those of [26], show substantial difference.

We have found explicit structure of the hysteresises, their total numbers and characteristics as functions of parameters of the system and driving radiation, and their relations to QS's. Furthermore, we found that while sharp boundaries of plasma layer contribute to the effect, they are not essential: layers with "soft" boundaries still exhibits all the major features of the phenomenon, providing its fundamental manifestation; they are also much more realistic ob-

jects for laboratory experiments or astrophysical observations. The major new and fundamental effect is that the phenomenon persists even for *semi-infinite* plasma with a small absorption, which also develops a strong retro-reflection. The "Sommerfeld condition" (no wave comes from the "infinity") is to be revisited here: a wave *is back-reflected* deep inside the plasma and comes to the boundary. Interfering with a forward wave, it results in a semi-standing wave, trapped QS's, and multistability, same as in a finite layer. The energy accumulated in QS's and excited free electrons, can then be released if plasma density reduces, as it may happen, e. g. in an astrophysical environment.

2. Nonlinear relativistic wave equation and boundary conditions

The wave propagation here is governed by a so called nonlinear Klein-Gordon-Fock equation:

$$[\nabla^2 - \partial^2/(\mathbf{v}\partial t)^2]\psi = k_0^2 f(|\psi|^2)\psi; \quad f(0) = 1. \quad (1)$$

where $f(|\psi|^2)$ is a function responsible for nonlinearity. Here, a generic variable, ψ , could be a scalar (e.g. a wave function in relativistic quantum mechanics, RQM), or a field vector in EM-wave propagation, \mathbf{v} is a scale velocity, ($\mathbf{v} = \mathbf{c}$ for plasma and in RQM), and k_0^{-1} is a spatial scale of the problem, (for RQM, $k_0 = m_0c/\hbar = 2\pi/\lambda_C$, where λ_C is the Compton wavelength, and m_0 is the rest-mass of an electron); for plasma $k_0 = \omega_{pl}/c$, where ω_{pl} is a plasma frequency due to free-charge density, ρ_e , and in the X-ray physics, $k_0 = E_{ph}/\hbar c$ is related to photo-ionization limit, E_{ph} , of atoms. For an ω -monochromatic wave $\vec{\psi} = \vec{\mathcal{E}}(\vec{r}) e^{-i\omega t}/2 + c.c.$, where $\vec{\mathcal{E}}(\vec{r})$ is a complex amplitude, using $u^2 = |\mathcal{E}|^2$. We will be using here a dimensionless amplitude $\mathcal{E} = E/E_{nl}$ with E_{nl} being some characteristic nonlinear scale, and for a RL-mass-effect this scale is $E_{nl} = E_{rl} = \omega m_0 c/e$, where m_0 is rest electron mass, so that amplitude u will be expressed in RL-units too $u = |E|/E_{rl}$. Equation (1) is now reduced to a nonlinear Helmholtz equation:

$$\nabla^2 \mathcal{E} + k^2 \varepsilon(u^2) \mathcal{E} = 0; \quad \varepsilon_{pl} = 1 - \omega_{pl}^2(u^2)/\omega^2 \quad (2)$$

where $k = \omega/c$, $\omega_{pl}^2 = 4\pi e\rho_e/m$ is a plasma frequency, with mass m being amplitude-dependant. In general, nonlinear dielectric constant ε may be due to quite a few factors, like varying ionization rate, plasma waves, ponderomotive force, etc. [7-9]. Assuming fully ionized gas, $\rho_e = const$, and a circularly-polarized wave, $\mathcal{E}(\zeta) (\hat{e}_x + i\hat{e}_y) e^{-i\omega t}/2 + c.c.$, that has negligible high-harmonics generation and minimal longitudinal plasma waves excitation, the most basic remaining source of nonlinearity is a field-induced RL mass-effect of electron: $m = m_0\gamma$, with a RL-factor $\gamma = \sqrt{1 + (p/m_0c)^2}$, where p is the momentum of electron. Since $p = um_0c$, (see e. g. [17-19]) we have $\gamma = \sqrt{1 + u^2}$ so that a relativistic dielectric constant, ε_{rl} , is

$$\varepsilon_{rl} = 1 - [v^2\gamma(u^2)]^{-1} \quad \text{with} \quad v = \omega/(\omega_{pl})_0 \quad (3)$$

where $(\omega_{pl})_0$ is a linear plasma frequency with $m = m_0$. Since $m = m(u^2)$, a single electron exhibits large hysteretic cyclotron resonance predicted in [27] and observed in [28]. The mass-effect has also become one of the major players in the multi-photon nonlinear optics of single electrons [25,29,30] as well as in light-plasma interaction [7-15], e. g. in RL self-focusing, and in acceleration of electrons by the beat-wave [31] and wake-field. The EM-propagation could also be accompanied by RL-intrinsic bistability [32-34].

In a 1D-case, letting a plane EM-wave propagate in the z -axis, we have $\nabla^2 = d^2/dz^2$. For semi-infinite dielectrics, a EM-wave incident from a dielectric with $\varepsilon = \varepsilon_{in} > 0$ under the angle θ onto a material of $\varepsilon = \varepsilon_{NL} > 0$, ε in Eq. (2) is replaced by $\varepsilon_{in}[\varepsilon_{NL}(\omega)/\varepsilon_{in}(\omega) - \sin^2\theta]$. For a microwave (*mw*) waveguide with a critical frequency ω_{wg} , ε in Eq. (2) is replaced by $\varepsilon_{wg}(1 - \omega_{wg}^2/\omega^2)$. The crossover point is attained at $\varepsilon = 0$. Equation (2) reduces then to

$$\mathcal{E}'' + \varepsilon(\zeta, u^2)\mathcal{E} = 0, \quad (4)$$

where $\zeta = kz$, and "prime" denotes $d/d\zeta$; in general, we do not assume ε *uniform* in ζ -axis. In a weakly-nonlinear media one can break the field into counter-propagating traveling waves and find their amplitudes *via* boundary conditions. However, near a crossover point one in general cannot distinguish between those waves. To make no assumptions whether a wave is traveling, standing, or mixed, we represent the field using real variables u , and phase (eikonal), ϕ , as

$$\mathcal{E} = u(\zeta)\exp[i\phi(\zeta)]. \quad (5)$$

Since \mathcal{E} is in general complex, while $\varepsilon = \varepsilon(u^2)$, Eq. (4), is isomorphous to a 3-rd order equation for u ; yet, it is fully integrable in quadratures. Its first integral is a scaled momentum flux

$$P \equiv u^2\phi' = inv. \quad (6)$$

In a lossless media P is conserved over the entire space $\zeta < \infty$, even if the medium is non-uniform, multi-layered, linear and/or nonlinear, etc. If a layer borders a dielectric of $\varepsilon = \varepsilon_{ex}$ at the exit, we have $P = u_{ex}^2\sqrt{\varepsilon_{ex}}$, where u_{ex}^2 is the exit wave intensity. Equation (4) is reduced then to a 2-nd order equation for u :

$$u'' + u[\varepsilon(\zeta, u^2) - P^2/u^4] = 0, \quad (7)$$

which makes an unusual yet greatly useful tool. Since it deals only with a real amplitude and uses flux P as a parameter, Eq. (7) is nonlinear even for a *linear propagation*, yet is still analytically solvable if a density ρ_e is uniform across the layer ($\partial\varepsilon/\partial\zeta = 0$). A full-energy-like invariant of Eq. (7) is

$$u^2/2 + U(u^2) = W = inv, \quad \text{with } U = \frac{1}{2} \left[\int_0^{u^2} \varepsilon(u^2) d(u^2) + P^2/u^2 \right], \quad (8)$$

where $u^2/2$ is "kinetic", and U – "potential" energies. For a RL-nonlinearity, Eq. (3), we have

$$U(u^2) = (u^2 + P^2/u^2)/2 - [\gamma(u^2) - 1]/v^2. \quad (9)$$

Here W is a scaled free EM energy density of ε -nonlinear medium [35] $W = c[H^2 + \int \varepsilon d(E^2)]/(2E_{rl}^2)$, where H is magnetic field. If a layer exit wall is a dielectric, one has $W = U(u_{ex}^2)$, since then $u'_{ex} = 0$ (see below). For a metallic mirror, $W = u_{ex}'^2/2$, since now $u_{ex} = 0$; and $W = 0$ for an evanescent wave in a semi-infinite medium. The implicit solution for spatial dynamics of u in general case is found now as

$$\zeta = \int \{2[W - U(u^2)]\}^{-1/2} du. \quad (10)$$

Boundary conditions at the borders with linear dielectrics at the entrance, $\zeta = 0$, with $\varepsilon = \varepsilon_{in}$, and at the exit, $\zeta = d$, with $\varepsilon = \varepsilon_{ex}$, result in complex amplitudes of incident, \mathcal{E}_{in} , and reflected, \mathcal{E}_{rfl} , waves at $\zeta = 0$:

$$\mathcal{E}_{in,rfl} = [u \pm \varepsilon_{in}^{-1/2}(P/u - iu')]/2; \quad (11)$$

where "+" corresponds to \mathcal{E}_{in} , and "–" – to \mathcal{E}_{rfl} . At the exit point, $\zeta = d$, we have $u = \mathcal{E}_{ex} \equiv u_{ex}$; $u' = 0$; and $\phi' = \sqrt{\varepsilon_{ex}}$. A condition $P = 0$ corresponds to full reflection, resulting in either strictly standing wave, or nonlinear evanescent wave in a semi-infinite plasma, in particular in a "standing" soliton-like solution (see below). If $\varepsilon(u^2 = 0) < 0$, there are no *linear* traveling waves. Yet a purely traveling *nonlinear* wave may exist at sufficiently strong intensity $u^2 = u_{trv}^2 = const$, such that $\varepsilon(u_{trv}^2) > 0$:

$$\mathcal{E}_{trv} = u_{trv}\exp(i\phi'\zeta), \quad \phi' = \pm\sqrt{\varepsilon(u_{trv}^2)}, \quad (12)$$

propagating either forward (+) or backward (-). However, if $\varepsilon(u=0) < 0$, it is strongly unstable. A non-periodic solution of Eq. (7) with $P = 0$ is a nonlinear evanescent wave that forms a standing, trapped soliton. In low-RL case, one needs a small detuning from crossover point, $\delta \equiv 1 - v \ll 1$, to attain the effect at low laser intensity, $u^2 \ll 1$, so that the dielectric constant, Eq. (4), is Kerr-like and small: $\varepsilon_{rl} \approx -2\delta + u^2/2$, $|\varepsilon_{rl}| \ll 1$. A full solution of Eq. (7) with $P = 0$ and $u \rightarrow 0$ at $\zeta \rightarrow \infty$ yields then a standing soliton with a familiar intensity profile:

$$u^2 = 8\delta / \cosh^2[(\zeta - \zeta_{pk})\sqrt{2\delta}] \quad (13)$$

where the peak location ζ_{pk} is an integration constant. For an arbitrary frequency, $v < 1$, the soliton peak intensity is

$$u_{sol}^2 = 4(1 - v^2)/v^4, \quad (14)$$

instead of 8δ as in Eq. (13); and

$$\varepsilon(u_{pk}^2) = (1 - v^2)/(2 - v^2) \geq 0. \quad (15)$$

When $v^2 < 1/2$, it is a strongly-RL soliton, $u_{sol}^2 \gg 1$, and its peak narrows down to a half-wave:

$$u^2 \approx u_{sol}^2 \cos^2(\zeta - \zeta_{pk}) \quad \text{at } u^2 > 1. \quad (16)$$

3. Finite layer plasma and quasi-solitons

In a finite layer one has a mix of standing/evanescent and traveling waves, with $u_{min}^2 = u_{ex}^2 = P > 0$. A full integration of Eq. (7) with nonlinearity $\varepsilon_{rl} \approx -2\delta + u^2/2$ yields then elliptic integrals of imaginary argument of the first kind; more importantly, Eq. (7), and its invariant avails themselves to detailed analysis. The numerical simulations are needed, however, to find a solution for (a) strongly-RL field [using Eq. (7) and its integrals], or (b) non-uniform plasma density in Eq. (7) (Section 4 below), or (c) plasma with absorption [Eq. (4) with v^2 replaced with $v^2(1 + i\alpha)$, where α is an absorption factor, Section 6 below). It is then found by an "inverse propagation" procedure, whereby we essentially back-track the propagation from a purely traveling exit wave back to the entrance. One sets first a certain magnitude of $u_{ex}^2 = P$, $u'_{ex} = 0$ at the exit, numerically computes an amplitude profile $u(\zeta)$ back to the entrance and incident and reflected intensities u_{ex}^2 and u_{rfl}^2 using Eq. (11), and then maps u_{ex}^2 and u_{rfl}^2 vs incident intensity, u_{in}^2 . A data set $u_{in}^2(P)$ and $u_{rfl}^2(P)$ for any given P is found then with a single run, vs a so called multi-shooting commonly used in search of solution with conditions set at two boundaries. This provides a very fast numerical simulation vs multi-shooting; besides, the latter one is very unreliable when dealing with apriory unknown number of multi-solutions.

For a fully-RL simulation with a $L = 10\lambda$, where L is the layer thickness, Fig. 1 show the emergence of large number, N_{hs} , of huge hysteretic loops of the transmission (same as in reflection, not shown here), which bounces between full transparency (near the points touching an FT line) to nearly full reflection (near the points touching an envelope NFR). In general, $N_{hs} = O(L/\lambda)$. In an unbound plasma, the solution of Eq. (7) with a traveling component, $P > 0$, is a spatially periodic and positively defined, with the intensity, $u^2(\zeta)$, bouncing between two limits, u_{ex}^2 , and u_{pk}^2 . If $P/16 \ll \delta^2 \ll 1$, we have

$$P = u_{ex}^2 \leq u^2 \leq u_{pk}^2 \approx 8\delta + P/2\delta \quad (17)$$

i. e. the peaks are relatively large, $u_{pk}^2 \gg u_{ex}^2$ and form a train of well separated QS's nearly coinciding with a standing soliton, Eq. (13), of the peak intensity $u_{pk}^2 \approx 8\delta$. As P and u_{in}^2 increase, they grow larger and closer to each other. The spatial period, Λ , of this structure is:

$$\Lambda/\lambda \approx \ln(16\delta/\sqrt{P})/(2\pi\sqrt{2\delta}) \quad (18)$$

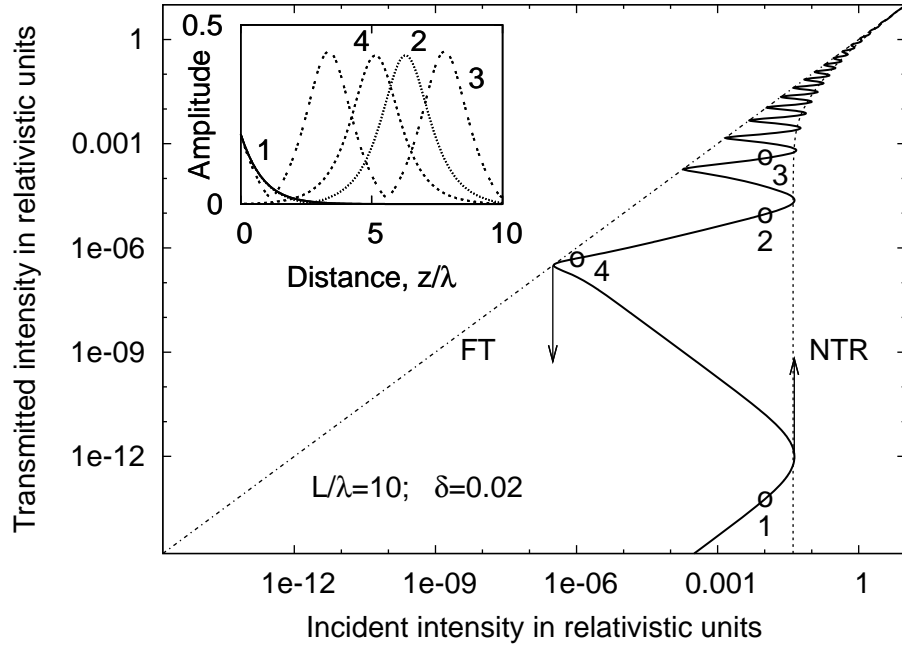


Fig. 1. Hysteretic transmission of light through a plasma layer of thickness L . **FT** and **NTR** are full transparency and near total reflection limits. Points 1, 2, 3 mark a linear evanescent wave, 1-st, and 2-nd upper stable states respectively, and 4 – a QS sustained by a very low pumping. Arrows indicate direction of jumps within the lowest hysteretic loop. Inset: spatial amplitude profiles of waves corresponding to points 1-4 in the main plot.

In a strongly RL case, $P > 1$, we have

$$u_{pk}^2/P \approx 1 + (1+P)^{-2}, \quad \text{and} \quad \Lambda \approx \lambda/2, \quad (19)$$

as for a standing, albeit inhibited wave component in free space, while traveling wave component emerges dominant, resulting in self-induced transparency.

4. Relativistic multi-hysteresises and immobile quasi-solitons

Hysteretic jumps occur when either valley or peak of the intensity profile coincide with an entrance, $\zeta = 0$. The valley, $u_0^2 = u_{ex}^2$, marks an off-jump in Fig. 1, and the peak, $u_0^2 = u_{pk}^2$ – an on-jump. Suppose that in a layer of $L > \lambda/(2\pi\sqrt{2\delta})$, the incident intensity u_{in}^2 is ramped up from zero. When $u_{in}^2 < 2\delta$, Fig. 1. point 1, the amplitude is almost exponentially decaying, $\zeta = 0$, as $u \approx 2u_{in} \exp(-\sqrt{2\delta}\zeta)$, i. e. is a nearly-linear evanescent wave, curve 1 in Fig. 1 inset; the layer is strongly reflective, and the transmission is low. As u_{in}^2 increases, the front end of that profile swells up, becoming a semi-bell-like curve, close to Eq. (13) with $\zeta_{pk} \approx 0$. With further slight increase of pumping, it gets unsustainable, and the field configuration has to jump up to the next stable branch of excitation, whereby it forms a steady QS at the back of the layer. If after that u_{in}^2 is pulled down adiabatically slow, the QS moves to the middle of the layer (Fig. 1. point 2, curve 2 in the inset). Finally, when it is exactly at the midlayer (Fig. 1. point 4, curve 4 in the inset), both valleys are at the borders of the layer, the pumping is nearly minimal to support a QS; below it the profile is unsustainable again, and the system jumps down to a regular nearly-evanescent wave and almost full reflection.

At this remarkable point, the layer is fully transparent, i. e. all the (very low) incident power is transmitted through, while a giant QS of peak intensity $(u_{in})_{pk}^2 \approx 2\delta$ inside the layer is sustained by a tiny incident power, $(u_{in})_{min}^2$. If $L\sqrt{2\delta}/N\lambda > 1$, the contrast ratio – essentially a nonlinear resonator’s finesse, Q , – can be tremendously high:

$$Q = \frac{(u_{in})_{pk}^2}{(u_{in})_{min}^2} \approx \frac{\exp(2\pi L\sqrt{2\delta}/N\lambda)}{128 \delta} \gg 1 \quad (20)$$

where N is the number of QS’s in a layer; the one with $N = 1$ occurs after the first jump-up. In the example for Fig. 1 ($\delta = 0.02$, $L = 10\lambda$), $Q \sim 10^7$. In semi-infinite plasma, Q is limited by absorption, see below. It also decreases as N increases; the field profile for $N = 2$, is depicted in Fig. 1, point 3, curve 3 in the inset. Only half of multi-steady-states are stable; the stability condition is that the EM-energy density increases with the pumping, i. e. $dW/d(u_{in}^2) > 0$, which also coincides with the condition $d(u_{ex}^2)/d(u_{in}^2) > 0$, similar to [1,2].

One can view a QS at a N -th stable branch as a N -th mode of a self-induced resonator, with full transparency points marking the resonance. The plot of transmission intensity, u_{ex}^2 , vs incident intensity, u_{in}^2 , Fig. 1, makes a multi-hysteretic curve, which bounces between full transmission (marked by **FT** line, whereby $u_{ex}^2 = u_{in}^2$, to near total reflection (**NTR**). The envelope of the latter one, i. e. the minimal transmitted intensity, $(u_{ex}^2)_{min}$ at each incident intensity, u_{in}^2 (both in relativistic units) has been approximately estimated by us as:

$$\frac{1}{(u_{ex}^2)_{min}} \approx \frac{1}{4(u_{in}^4 - 4\delta^2)} + \frac{1}{u_{in}^2} \quad (21)$$

so that the threshold for the first up-jump is $u_{in}^2 = 2\delta$, i. e. its respective amplitude is twice as small as the amplitude of the first excited ”half”-soliton, Eq. (13) (the total incident+reflected field is exactly double of the incident amplitude, and thus equal to that soliton amplitude). This result coincides with the one for a up-jump due to soliton formation at nonlinear interface [1,2].

5. No need for sharp boundaries!

In optical bistability based on a nonlinear Fabri-Perot resonator [36], the resonator mirrors determine the narrow resonances and thus are absolutely necessary for the existence of the effect. Sharp mirror boundaries of plasma layer [26] may enhance the resonances, but since those resonances are self-induced, we found that sharp mirror-like layer boundaries do not constitute necessary requirement: the same effect emerge even with the plasma density, ρ , varies smoothly in space, and vanishes completely at far edges of a plasma layer. Our numerical simulations using Eqs. (4) and (7), where we have now to make ε explicitly dependent on the distance ζ :

$$\varepsilon(\zeta, u^2) = 1 - \rho(\zeta)[\rho_0 v^2 \gamma(u^2)]^{-1} \quad (22)$$

showed that a layer with ”soft” shoulders making $\sim 50\%$ of the entire layer length, still exhibits a few hysteresises, and a large number of self-induced resonances. An example of this for $\delta = 10^{-4}$ is shown at Fig. 2, depicting transmitted and reflected wave intensities vs the incident wave intensity in the case whereby the plasma layer has a varying plasma density along the propagation path, which has a flat density distribution in the middle and tapers down to zero at the edges of the layer, see inset at Fig. 2. For numerical simulation purposes, a specific model profile chosen by us here is $\rho(z)/\rho_0 = 1$ at $|z| \leq L/2$,

$$\rho(z)/\rho_0 = \cos^2[\pi(|z| - L/2)/2S] \quad \text{at} \quad L/2 < |z| \leq L/2 + S \quad (23)$$

and $\rho(z) = 0$ elsewhere, where L is the thickness of a sub-layer with a flat distribution of plasma density, and S is the shoulder thickness; at the half-max of the density distribution

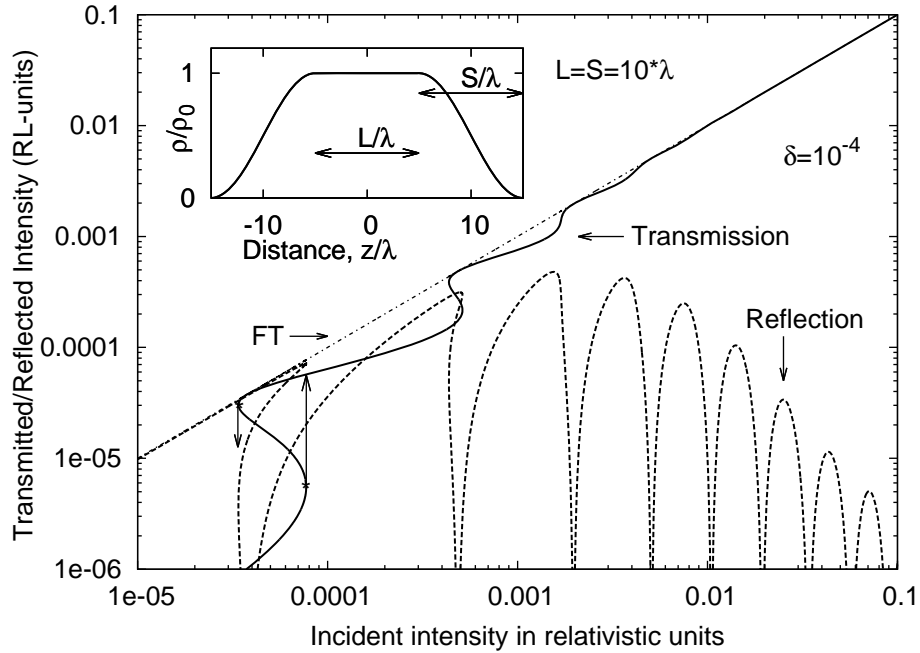


Fig. 2. Hysteretic transmission and reflection of light and multi-self-induced resonances at a plasma layer formed by a homogeneous, L -thick sub-layer, having plasma density ρ_0 , and two S -thick shoulders, with the plasma density, ρ , tapered smoothly to zero. **FT** marks full transparency. Inset: a spatial profile of normalized plasma density $\rho(z)/\rho_0$.

the layer is $L + S$ thick. In the example on Fig. 2, $L = S = 10\lambda$. One can see that even at such smoothly distributed plasma there is still two hysteresises (the largest one of them is indicated by vertical arrows) and multiple self-induced resonances. The formation of QS field spikes at the slopes density distribution here might be assisted by a linear so called "gradient marker" effect [38]. While the fact that smooth-distribution plasma layers can still produce multi-hysteresises and resonances is of great significance for the physics of such systems, it may be even more important for experimental observation of the phenomenon in "real life" systems, such as plasma jets in the lab, or the pancake-like slabs of plasma ejected from a star.

6. Multi-hysteresises in semi-infinite plasma with absorption

The fundamental manifestation of the phenomenon transpires in a *semi-infinite* plasma. Only two kind of waves [1,2] in a lossless case satisfy then the Sommerfeld condition – no wave "comes back" from $\zeta \rightarrow \infty$ – a traveling, Eq. (12), $du/d\zeta \rightarrow 0$, and an evanescent, Eq. (13), waves, $u \rightarrow 0$. Our preliminary investigation of Eq. (2) showed that the wave, Eq. (12), is unstable both in 2D&3D-propagation – and, of Eq. (1) – in temporal domain in 1D-case. However, using Eq. (4), in which a real term v^2 is replaced by a complex one:

$$v^2 \rightarrow v^2(1 + i\alpha); \text{ with } \alpha = (\omega\tau)^{-1} \quad (24)$$

where α is an absorption factor, and τ is an electron momentum relaxation time, one can show that even a *steady* 1D-wave, Eq. (12), does not survive small absorption, $\alpha \ll 1$. A condition for a hysteresis to emerge is then

$$\alpha < \alpha_{cr} \approx e\delta \text{ if } \delta \ll 1 \quad (25)$$

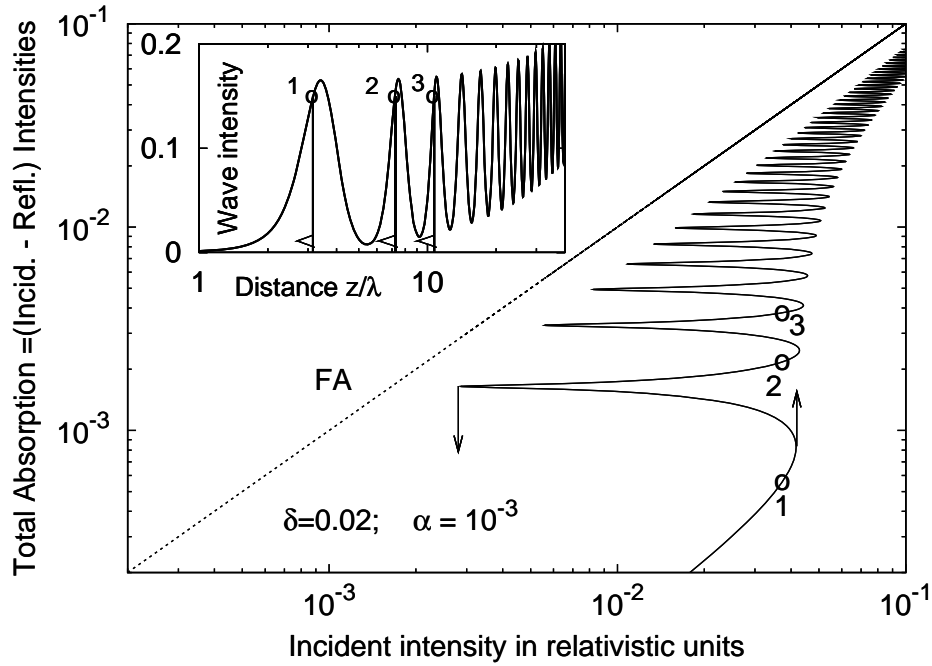


Fig. 3. Hysteretic absorption of light in a semi-infinite plasma layer with absorption $\alpha = 10^{-3}$. **FA** is a full absorption limit. Points 1, 2, 3 mark a linear evanescent wave, 1-st, and 2-nd upper stable states respectively. Arrows – the same as in Fig. 1. Inset: intensity profile; points and verticals 1-3 indicate locations of the plasma boundary for the respective points in the main plot; \triangleleft 's show direction into plasma layer.

where α_{cr} is a critical absorption [37]. Near $\alpha \sim \alpha_{cr}$, a jump-up occurs at $u_{in}^2 \approx \pi\delta$. The ratio, Eq. (20), to sustain a single QS is limited now by $Q \approx \delta/\alpha$, and can still be huge. If $\alpha \ll \alpha_{cr}$, the first jump still occurs at the incident intensity equal to a quarter of soliton, Eq. (13), intensity:

$$u_{in}^2 \approx 2\delta \quad (26)$$

When pumped hard, new QS emerge and move deeper into plasma. A question then is what is the spacing L_{spc} , between the most submerged ones, i. e. the maximum spacing between standing solitons in absorbing plasma. We found that the ratio "min/max" of the intensities is

$$u_{min}^2/u_{max}^2 \approx \alpha/\delta; \quad i. e. \quad u_{min}^2 \approx 8\alpha \quad (27)$$

Assuming that down to the bottom, the intensity follows very close to the soliton solution, Eq. (13), and making correction for the length of the "bottom", we estimate the spacing L_{spc} as

$$L_{spc} \approx k^{-1} \sqrt{2/\delta} [1 + \ln(\sqrt{\delta/\alpha})] \quad if \quad \alpha \ll \delta \ll 1 \quad (28)$$

which was confirmed by our numerical simulations. The QS's are well spaced and distinguished from each other if $\alpha \ll \delta$, which is a natural condition for the detuning δ to be set sufficiently far from the the cross-over point in the presence of non-zero absorption.

Hysteresises in reflection at $\alpha = 10^{-3}$ are shown in Fig. 3, and the intensity profile for $u_{in}^2 > 2\delta$ – in the inset. An initially traveling wave develops oscillations due to rising standing wave, which eventually becomes a train of trapped QS's, the last one being a QS close to Eq. (13), and

the field then vanishes exponentially. Reducing α pushes that last QS further back, but does not extinguish retro-reflection from the QS train at the crossover area deep inside plasma, keeping the condition $u \rightarrow 0$ at $\zeta \rightarrow \infty$. One has to note that while the effects described in Sections 3-5 can typically be observed in relatively thin, (i. e. a few λ thick) layers, where transverse self-action effects could be safely neglected, the use of a 1D-model for the light propagation in a semi-infinite plasma may not be adequate due to 3D self-focusing and channeling [39] and related instabilities [40]. Yet it is still of significance to know the tendency of behavior of such systems beyond critical condition, Eq. (25). The most important factor, however, is that there are many other nonlinear systems that can be adequately described by 1D-approach using Eq. (4), such as e. g. plasma waveguide or dielectric nonlinear waveguide whose linear parameters are such that they disallow weak wave propagation but can support the propagation of sufficiently powerful wave, with the transverse field distribution (in particular self-action) being only slightly affected by the nonlinearity.

7. Discussion

Lab experiment in thin plasma layer could be set up with e. g. jet of gas irradiated by a powerful CO_2 laser, with a gas density controlled to reach a crossover point at $\lambda_{CO_2} \approx 10\mu m$. This process may be also naturally occurring in astrophysical environment in plasma sheets expelled from a star (e. g. the Sun); part of the star's radiation spectrum below the initial plasma frequency is powerful enough to penetrate into the layer and be trapped as QS's. When the layer expands, they get released as a burst of radiation, similarly to bubbles in boiling water. It is also conceivable that the QS trapping and consequent release may be part of the physics of ball-lighting subjected to a powerful radiation emitted by the main lighting discharge in mw and far infrared domains. The QS's might be used e. g. for laser fusion to deposit laser power much deeper into the fusion pallets; or for heating the ionosphere layers by a powerful rf radiation.

8. Conclusions

In conclusion, optical multi-hysteresises may emerge in an overdense plasma near critical plasma frequency due to fundamental relativistic mass-effect of electrons alone. They may result in huge trapped, or standing quasi-solitons with the intensity greatly exceeding that of pumping radiation. The effect can manifest itself in finite plasma layers with both sharp and soft boundaries, as well as in a semi-infinite plasma with low absorption.

9. Acknowledgments

This work was supported by AFOSR.